

## The Dependence of Reaction Rates on the Surface Structure for Supported Nickel Catalysts

CLYDE S. BROOKS

*United Aircraft Research Laboratories, East Hartford, Connecticut 06108*

Received March 8, 1973; revised November 7, 1973

### NOMENCLATURE

$a$	External area of pellet, cm <sup>2</sup> /g	$r_e$	Effective pore radius, cm
$\bar{a}$	Ratio external surface to volume catalyst pellet	$S_v$	Space velocity = GRT/PZ cm <sup>3</sup> reactant vapor/cm <sup>3</sup> cat. sec
$(Bi)_h$	Biot number for heat transfer = $hL/\lambda$	$T$	Absolute temperature
$(Bi)_m$	Biot number for mass transfer = $k_c L/D_K$	$T_s$	Absolute temperature external surface of catalyst pellet
$C$	Reactant concentration, g mole/cm <sup>3</sup>	$\Delta T_x$	Temperature gradient in film external to catalyst pellet
$C_s$	Reactant concentration at surface of pellet, g mole/cm <sup>3</sup>	$\Delta T_0$	Total temperature change
$Da$	Damkohler number	$y_1$	Reactant concentration into catalyst bed
$D_{12}$	Bulk diffusion coefficient for binary mixture, cm <sup>2</sup> /sec	$y_2$	Reactant concentration from catalyst bed
$D_{eff}$	Effective pore diffusion coefficient for porous solid, cm <sup>2</sup> /sec	$Z$	Catalyst bed length, cm
$D_b$	Bulk pore diffusion coefficient, cm <sup>2</sup> /sec	$\epsilon$	Catalyst bed porosity, fractional
$D_K$	Knudsen pore diffusion coefficient, cm <sup>2</sup> /sec	$\eta$	Effectiveness factor
$dp$	Catalyst pellet diameter, cm	$\theta$	Catalyst pellet porosity, fractional = $\frac{1}{\rho_B} - \frac{1}{\rho_S}$
$G$	Mass flow velocity, g mole/cm <sup>2</sup> sec	$\lambda$	Thermal conductivity, cal./sec cm deg. cent.
$\Delta H$	Heat of reaction, Kcal/mole	$\mu$	Viscosity, poise
$h$	Heat transfer coefficient in film around catalyst pellet, cal/cm <sup>2</sup> sec	$\rho$	Vapor density, g/cm <sup>3</sup>
$k_c$	Mass transfer coefficient in film around catalyst pellet = $k_p RT$	$\rho_B$	Bulk density of catalyst pellet, g/cm <sup>3</sup>
$k_g$	Bulk mass transfer coefficient, g mole/atm cm <sup>2</sup> sec	$\rho_S$	Skeletal density of catalyst pellet, g/cm <sup>3</sup>
$L$	Volume to external surface ratio of catalyst pellet $1/\bar{a}$	$\sigma_{12}$	Lennard-Jones force constant (Å)
$M_1, M_2$	Molecular weight species 1 and 2	$\tau$	Pore tortuosity
$M_m$	Average molecular weight of diffusing reactant	$\Omega_D$	Collision integral
$P$	Total pressure, atm		
$P_f$	Pressure film factor, atm		
$P_g$	Partial pressure of reactant in bulk vapor stream, atm		
$P_i$	Partial pressure of reactant at surface of catalyst pellet, atm		
$R$	Gas constant		
$R_0$	Experimental reaction rate, mole/g cat. sec		
$r$	Ratio of Biot numbers $(Bi)_m$ for mass and $(Bi)_h$ for heat transfer		

An examination has been made of the dependence of observed reaction rates on the accessibility of the catalytic surface of supported nickel catalysts. Catalyst properties which are required in order to relate quantitatively experimental reaction rates to catalyst surface structures consist of porosity (pellet and catalyst bed), pellet size and geometry, effective pore size within the catalyst pellet, and reactant pore diffusion coefficients. The present example consists of the heterogeneous reaction of water vapor and *n*-hexane to form hydro-

gen and carbon dioxide over nickel supported on alumina and synthetic zeolites (synthetic mordenite and faujasite). Mass transfer coefficients for bulk diffusion to the catalyst pellet, pore diffusion coefficients, external and internal temperature gradients, and effectiveness factors were calculated to provide insight into the effect of heat and mass transport in micropore structures on the observed reaction rates.

The zeolite supported nickel catalysts demonstrate outstanding activity for steam reforming of *n*-hexane in the temperature range of 400° to 500°C at one atmosphere. The fine pore structure of these catalysts provides a much greater limitation on mass transport via pore diffusion and a predominance of heat transfer at the external surface of the catalyst pellets in contrast to the more conventional nickel alumina catalyst.

#### INTRODUCTION

The purpose of this paper is to demonstrate how the significant factors in surface structure have a bearing on reaction kinetics and the procedures used for their experimental determination. Selection of significant quantitative criteria for guidance in design of catalyst structures is the ultimate practical objective.

Supported nickel catalysts provide examples of how surface structure parameters can be used to relate surface structure to reaction kinetics. The reaction selected is the steam reformation of *n*-hexane to hydrogen and carbon dioxide over nickel supported on alumina and zeolites.

The kinetic parameters used in this paper consist of the experimental reaction rates, the external (molecular) diffusion coefficients for the reactant to the external surface of the catalyst pellets, the pore diffusion coefficients (bulk and Knudsen) and the effectiveness factors. In addition, the temperature gradients in the external film and within the catalyst pellet were calculated.

These parameters permit definition of limitations on mass and heat transfer due to reactant diffusion to the external catalyst pellet surface and within the pores of

the catalyst pellets. The ultimate objective is to establish the role of bulk molecular and pore diffusion and heat transfer effects in determining the observed reaction rates.

For the sake of the present data treatment, reaction is considered to be first order. If the initial data evaluation establishes to a first approximation that external bulk and internal pore diffusion limitations do not affect the observed reaction rates, the experimental rate data should represent intrinsic reaction rates. In this latter case, effort is then justified in order to design more refined kinetic relationships for the given reaction. Perhaps most important of all, these kinetic relationships provide a quantitative basis to permit optimum design of catalyst pellet structure. This approach should be especially applicable to the high surface area, supported metal catalysts in which the reactive catalytic surface lies almost entirely in micropores ( $< \approx 300 \text{ \AA}$ ).

The information essential for definition of the selected kinetic parameters consists of the porosity (pellet and catalyst bed), pellet size and geometry, effective pore size within the catalyst pellet, thermal conductivity and reactant diffusion coefficients (bulk and Knudsen).

Additional structural information relevant to reaction kinetics and useful for catalyst pellet design consists of the specific surface area of the pellet, accessible catalytic metal surface area, surface morphology and elemental composition. Surface morphology should include catalytic metal size and shape, pore size distribution within the catalyst pellet, and the crystallography of the catalytic metal and the support. The elemental composition of primary concern is that of the pellet surface, initially and as modified by the reaction of interest.

#### EXPERIMENTAL RESULTS

##### *Catalyst Properties*

A summary of the relevant properties of the nickel alumina and nickel zeolite catalysts are summarized in Table 1.

Zeolites provide the opportunity for

TABLE 1  
 CATALYST PROPERTIES

Catalyst	Metal content (Wt. %)	Total area BET N <sub>2</sub> (m <sup>2</sup> /g)	Metal area by CO chemisorption (m <sup>2</sup> /g cat. <sup>a</sup> )	Porosity		r <sub>e</sub> Av. pore radius (Å)
				Total cm <sup>3</sup> /g	<300 Å Pore radius (cm <sup>3</sup> /g)	
Nickel-alumina (Girdler G56)	14.5	39	10	0.260	0.126	133
Nickel mordenite	3.24	297	30	0.540	0.54	36
Nickel Y faujasite (Linde SK400)	0.76	625	0.97	0.749	0.75	24

<sup>a</sup> After reduction in hydrogen at about 450°C. Assumed cylindrical shape  $r_e = \frac{2(\text{porosity})}{(\text{area})}$ .

preparation of a highly disperse catalytic metal phase at low metal loading by ion exchange compared with the relatively large metal particle sizes at higher metal loading than obtained with conventional solution impregnation, such as for nickel on alumina.

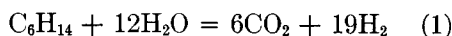
The zeolites provide high porosity within the matrix of crystalline cages, combined with small (7–10 Å) access pores. The average pore sizes reported in Table 1 are based on the total surface area and total pellet porosity and are much larger than the zeolite cage access pores because the macropore structure between zeolite crystallites is included.

Another interesting feature of the nickel zeolite catalysts is that even with an accessible catalytic metal area comparable or greater than that of a solution impregnated nickel alumina system, there is a very extensive exposure of the zeolite substrate. This is of particular interest when the substrate provides a catalytic role, such as surface acid sites to form a dual functional catalyst.

#### Reaction Rates for Steam Reformation of *n*-Hexane

The illustrative example presented here consists of the steam reformation of *n*-hexane to hydrogen and carbon monoxide over nickel catalysts. This reaction was conducted over the temperature range 400° to 500°C at a total pressure of one atmosphere. The reaction of *n*-hexane with steam

for conversion to hydrogen and carbon dioxide is given by the equation



A steam to carbon atom ratio of 2:1 is maintained to minimize the formation of carbon monoxide as an intermediate product and carbon deposition on the catalyst. The experimental procedures and reaction rate data have been published in detail elsewhere (1).

It is evident from comparison of the observed reaction rates expressed as micromoles of *n*-hexane reacted per gram of catalyst per second and as micromoles of *n*-hexane reacted per gram of catalytic metal per second that the zeolite catalysts, which have a higher state of metal dispersion than the nickel on alumina catalyst, provide greater specific catalytic activity (columns 4 and 5, Table 2).

This enhanced specific activity can be attributed at least in part to the more extensive catalytic metal surface in the case of the mordenite catalysts. This is evident from examination of the chemisorption metal areas of these catalysts (column 4, Table 1). The zeolite substrate provides the means of creating the highly disperse nickel catalytic surface which plays the significant role in this enhanced activity. In addition, the surface hydrogen on the zeolite may play a catalytic role by introducing a cracking function.

The faujasite catalyst, for example, has substantially less total available metal

TABLE 2  
EXPERIMENTAL REACTION RATES FOR STEAM REFORMATION  
OF *n*-HEXANE OVER SUPPORTED NICKEL CATALYSTS<sup>a</sup>

Catalyst	Temperature (°C)	$S_v$ (cm <sup>3</sup> <i>n</i> -hexane vapor/cm <sup>3</sup> catalyst hr)	$R_0$ (reaction rate)		
			$\mu$ moles/g catalyst sec	$\mu$ moles/g nickel sec	mole H <sub>2</sub> O/ carbon atom
Nickel alumina	400	4120	0.71	4.8	2.2
	428	244	0.26	1.8	2.4
	500	1880	0.28	2.0	2.5
Nickel mordenite	400	2950	0.83	24.0	2.2
	441	556	0.60	18.4	2.4
	500	3660	0.54	17.0	2.5
Nickel Y faujasite	412	560	0.60	60.2	2.4

<sup>a</sup> 1 atm total pressure.

area per unit weight than the nickel-alumina catalyst, yet it provides a greater specific catalytic activity.

The other conclusion that is evident from the reaction rates in columns 4 and 5 of Table 2 is that there is a decrease, rather than an increase in the observed rate in raising the temperature 30° to 40°C from 400°C and decreasing the fuel space velocity. Further increases in temperatures of 70° and 60°C, respectively, accompanied by an increase in space velocity lead to essentially no change in rates. This demonstrates that there is a strong limitation, due to mass transport effects for both the nickel-alumina and nickel mordenite catalysts.

In view of the extensive micropore structure of the zeolite catalysts, it is of interest to consider the limitations imposed on mass transport in and out of the catalyst pellets, due to reactant diffusion in the pores.

#### KINETIC PARAMETERS

The calculations are presented here for the kinetic parameters: bulk diffusion coefficients, pore diffusion coefficients, effectiveness factors, and temperature gradients.

##### *External Diffusion*

The bulk diffusion coefficient for a binary mixture can be calculated from the Lennard-Jones relation, Eq. 2 (2), in the absence of values determined experimentally.

$$D_{12} = \frac{0.001858T^{3/2}[(M_1 + M_2)/M_1M_2]^{1/2}}{P\sigma_{12}^2\Omega_D} \quad (2)$$

where  $T$  is absolute temperature,  $M_1$  and  $M_2$  are molecular weights of the two components,  $P$  is total pressure in atmospheres,  $\sigma_{12}$  is the force constant and  $\Omega_D$  is the collision integral.

The pressure difference between the bulk phase of the reactant stream and the external surface of the catalyst pellets in a fixed bed catalyst in a tubular reactor can be calculated from the relation, Eq. 3 (3),

$$P_i - P_g = \frac{R_0 M_m P_f (\mu/\rho D_{12})^{2/3}}{1.82aG(\text{dp}G/\mu)^{-0.51}} \quad (3)$$

Once the pressure differential ( $P_i - P_g$ ) is calculated, the diffusion rate coefficient for external diffusion to the catalyst pellet can be calculated from the relation

$$kg = \frac{R_0}{a(P_i - P_g)} \quad (4)$$

Employing Eq. (3) for the estimation of the differential in reactant partial pressure due to external diffusion at the catalyst pellet external surface, the calculated  $P_i - P_g$  values were determined to be quite small, amounting to less than one percent for both the nickel-alumina and the nickel mordenite catalysts. Only the nickel faujasite zeolite gave a  $P_i - P_g$  value in excess of 1% (column 4, Table 3). In addition, the mass transport coefficient,  $k_g$ , for

TABLE 3  
DIFFUSION CALCULATIONS FOR *n*-HEXANE STEAM REFORM REACTION

Catalyst	Temperature °C	$G_m$ micromoles/ cm <sup>2</sup> sec	External diffusion		Pore diffusion coefficient (cm <sup>2</sup> /sec = 10 <sup>4</sup> )	
			$P_i - P_g$ [Eq. (3)]	$k_g$ μmoles/ cm <sup>2</sup> sec atm [Eq. (4)]	$D_b$ [Eq. (5)]	$D_K$ [Eq. (6)]
Nickel alumina	400	356	0.00271	36.5	648	65.4 <sup>a</sup>
	428	20.2	0.00392	9.2	703	66.4 <sup>a</sup>
	500	318	0.00106	36.9	855	70.1 <sup>a</sup>
Nickel mordenite	400	432	0.00123	40.4	542	4.13 <sup>b</sup>
	441	21	0.00399	8.92	608	4.23 <sup>b</sup>
	500	178	0.00115	28	715	4.42 <sup>b</sup>
Nickel Y faujasite	412	20.9	0.0169	5.04	616	4.59 <sup>b</sup>

<sup>a</sup>  $\tau = 3.74$ .

<sup>b</sup>  $\tau = 4$ .

this faujasite catalyst (column 5, Table 3) is appreciably smaller than those calculated for the other two catalysts. This can probably be attributed to the relatively large pellet size (0.476 cm radius) of the faujasite catalyst, compared with the 0.16 cm radius pellet size of the nickel-alumina and nickel mordenite catalysts.

#### Pore Diffusion

The diffusion of reactant within the pores of the catalyst pellet can be due to either bulk diffusion

$$D_{\text{bulk}} = D_{12}\theta/\tau \quad (5)$$

in the case of large pores at moderate to high pressures, or to Knudsen diffusion.

Knudsen diffusion coefficients can be calculated from the equation

$$D_{\text{Knudsen}} = \left( 9700r_p\theta \sqrt{\frac{T}{M_m}} \right) / \tau \quad (6)$$

Knudsen diffusion dominates at low pressures ( $\approx 1$  atm) and in small pores ( $< \approx 300$  Å radius).

The relationship of pore structure to mass transport in the pores of catalysts has been examined in considerable detail by Wheeler (4, 5) and more recently by Satterfield (6).

The tortuosity term,  $\tau$ , which appears in Eqs. (5) and (6), accounts for variations in the shape and straightness of the pores. Examination of the considerable number of

$\tau$  values determined experimentally (6, Chap. 1) shows that for the most part the  $\tau$  values lie within a range of 2 to 6.

Appropriate bulk diffusion coefficients,  $D_{12}$ , can be used in conjunction with Knudsen diffusion coefficients,  $D_k$ , to calculate the effective diffusion coefficient ( $D_{\text{eff}}$ ).

Comparison of the bulk and Knudsen diffusion coefficients calculated for the zeolite catalysts demonstrates that the Knudsen diffusion coefficients are of the order of one-hundredth the bulk values and, hence, will almost exclusively determine the mass transport rates within the catalyst pellets (columns 6 and 7, Table 3).

The Knudsen diffusion coefficients are of the order of one-tenth the bulk diffusion coefficients calculated for the nickel alumina catalyst, indicating that for the catalyst Knudsen diffusion also will dominate. The Knudsen diffusion coefficients for pore diffusion were calculated from Eq. (6), using the intralattice pore radius of 10 Å characteristic of the mordenite and faujasite zeolites and not the average pore radii, 36 and 24 Å, respectively, calculated from the porosity and surface area for the mordenite and faujasite zeolites (column 7, Table 1).

The Knudsen pore diffusion coefficients for the zeolites are significantly less than for the larger pore size alumina support system, but not nearly as small as might

be expected for the small pore size zeolites. There is essentially no published information on systems directly comparable to those reported here, but diffusion coefficients of the order of  $10^{-9}$  cm<sup>2</sup> sec<sup>-1</sup> at 300°–540°C have been reported for *n*-hexane in offretite which has quite small pores (3.7 to 4.1 Å) (7).

A new theoretical treatment for the calculation of diffusivity and effectiveness factors in zeolites has been proposed by D. M. Ruthven (8), but to date no application of this theory has been made to experimental data.

The average pore radius used for the nickel-alumina catalyst was the 133 Å calculated from the experimentally determined surface area and porosity.

These calculations provide confirmation that for a reaction conducted at a pressure of 1 atm in catalysts for which the active surface is primarily within a microporous structure, the Knudsen diffusion will dominate mass transport within the catalyst pellet.

#### Effectiveness Factors

The role of internal pore diffusion limitations on the availability of the catalytic surface for reaction can be evaluated from the effectiveness factors (6, Eq. 3.39, p. 148)

$$\eta = \frac{9(1 - \varepsilon)D_{\text{eff}}}{(dp/2)^2 \ln(y_1/y_2)S_v} \quad (7)$$

Relatively high space velocities, which produce reactant conversions less than 30%, are necessary to provide experimental rate data adequate for effectiveness factor calculations.

The calculated effectiveness factors (column 4, Table 4) demonstrate the extent to which pore diffusion effects limit the accessibility of the catalyst surface for chemical reaction. The zeolite catalysts yield effectiveness factors less than 0.1 in all instances and indicate that these catalysts must provide a much greater specific reactivity compared with the nickel-alumina in order to provide greater reaction rates (column 4, Table 2).

TABLE 4  
EFFECTIVENESS FACTORS FOR STEAM  
REFORMATION OF *n*-HEXANE OVER  
SUPPORTED NICKEL CATALYSTS

Catalyst	Temper- ature (°C)	Mass velocity (G) (μmoles/ cm <sup>2</sup> sec)	η effective- ness factor [Eq. (8)]
Nickel alumina	400	356	0.54
	500	318	0.25
Nickel mordenite	400	432	0.011
	500	178	0.037

#### Temperature Gradients

An important consideration in using the effectiveness factor is that application of Eq. (7) assumes isothermal conditions in the catalyst bed. A calculation of the temperature gradient within a catalyst pellet can be made from the heat of reaction, effective diffusion coefficient, thermal conductivity of the catalyst, and the reactant concentration gradient within the catalyst pellet.

$$T - T_s = \frac{(-\Delta H)(D_{\text{eff}})(C_s - C)}{\lambda} \quad (8)$$

This relationship was developed by Damkohler (9) and the scope of its applicability broadened by Prater (10).

Temperature gradients were calculated from Eq. (8), employing published data on the heat of reaction and thermal conductivity and  $D_{\text{eff}}$  values calculated from Eq. (6), assuming the reactant concentration on the interior of the catalyst pellet to approach zero. None of the supported nickel catalysts show significant temperature gradients ( $T - T_s$ ) indicating that isothermal reaction conditions are approximated within the catalyst pellets in the experimental data cited here (Table 5).

More recently Carberry *et al.* (11, 12) and Lee and Luss (13) have observed that whereas the gradients in reactant concentration occur primarily within the pores of the catalyst pellets, the gradients in temperature occur primarily in the external film at the outer surface of the catalyst pellets.

TABLE 5  
 TEMPERATURE GRADIENTS WITHIN CATALYST PELLETS<sup>a</sup>

Catalyst	Heat of reaction (kcal/mole)	$C_s$ ( $\mu$ gram mole/cm <sup>3</sup> )	$T_s$ (°C)	$T - T_s$ [Eq. (9)]
Nickel alumina	186.87	0.301	400	-0.74
	189.83	0.953	500	-2.5
Nickel mordenite	186.87	0.410	400	-0.063
	189.83	0.800	500	-0.13
Nickel Y faujasite	186.87	0.200	412	-0.034

<sup>a</sup> C assumed to be 0 within pellet;  $\lambda$  assumed to be  $5 \times 10^{-4}$  cal/sec cm deg C.

Carberry (14) has proposed a relationship which expresses the ratio of the temperature change in the external film,  $\Delta T_x$ , to the total temperature change,  $\Delta T_0$ , entirely in terms of parameters which can be determined experimentally.

$$\frac{\Delta T_x}{\Delta T_0} = \frac{r(\bar{\eta}Da)}{(1 + (\bar{\eta}Da)(r - 1))} \quad (9)$$

Here  $r$  is the ratio of the Biot numbers for mass

$$(\text{Bi})_m = \frac{K_c L}{D_K} \quad (10)$$

and for heat

$$(\text{Bi})_h = \frac{hL}{\lambda} \quad (11)$$

The ratio,  $r$ , can be expected to range from 10 to  $10^5$ . In the present case, the  $r$  ratios were estimated to range from  $\approx 7.72$  to 139 (Table 6, column 8). Experimental

heat transfer coefficients,  $h$ , are not available for the present system, but  $h$  can be expected to lie within the range  $\approx 0.02$  to  $0.2$  cal/cm<sup>2</sup> sec for forced convection flow through tubular reactors packed with catalyst pellets (15, 16, 17).

The product,  $\bar{\eta}Da$ , can be conveniently evaluated from the relationship

$$\bar{\eta}Da = \frac{R_0 a}{k_g} \quad (12)$$

The calculations based on Eq. (9) demonstrated that  $\Delta T_x/\Delta T_0$ , the ratio of the temperature change at the external surface of the catalyst pellets to the total temperature change, lies within the range of 0.32 to 0.56 for the nickel alumina and within a range of 0.98 to 0.99 for the nickel zeolites (Table 6, column 9).

Employing the relationships for calculation of internal [Eq. (8)] and external [Eq. (9)] temperature gradients, it is evi-

 TABLE 6  
 EXTERNAL TEMPERATURE GRADIENTS AROUND CATALYST PELLETS

Catalyst	$T_s$ (°C)	$k_g$ mass transfer coefficient ( $\mu$ moles/cm <sup>2</sup> sec atm) [Eq. (4)]	$a$ external area (cm <sup>2</sup> /g)	$\bar{\eta}Da$ [Eq. (12)]	$(\text{Bi})_m$ [Eq. (10)]	$(\text{Bi})_h^a$ [Eq. (11)]	$r =$ $(\text{Bi})_m/(\text{Bi})_h$	$\Delta T_x/\Delta T_0$ [Eq. (9)]
		Nickel-alumina	400	36.5	7.16	0.139	309 L	40 L
	500	36.9	7.16	0.0543	334 L	40 L	8.35	0.32
Nickel mordenite	400	40.4	16.74	0.345	5570 L	40 L	139.0	0.99
	500	28.0	16.74	0.323	4030 L	40 L	101.0	0.98
Nickel Y faujasite	412	5.04	7.05	0.839	617 L	40 L	15.4	0.99

<sup>a</sup>  $h = 0.02$  cal/cm<sup>2</sup> sec.

dent that within the limits of available data there are no significant temperature gradients within the catalyst pellets but principally at the external surface of the pellets.

### CONCLUSION

The objective of this paper has been to provide a clear illustration of how experimental reaction rates can be quantitatively related to catalyst surface structure for supported nickel catalysts. The example offered is that of steam reformation of *n*-hexane to hydrogen and carbon monoxide over nickel supported on alumina and two zeolites (mordenite and faujasite).

The kinetic parameters used to establish this relationship consist of external (bulk) diffusion coefficients, pore diffusion coefficients (bulk and Knudsen), effectiveness factors, and thermal gradients. These parameters quantitatively related observed reaction rates to catalyst pellet structure and size, pore diffusion, and heat transfer effects.

Computation of these kinetic parameters requires the following experimental or calculated values for the catalyst pellets: pellet size and geometry, porosity, effective pore radius, and diffusion coefficients (bulk and Knudsen). Also required are experimental or calculated values for thermal conductivity, porosity, temperature of the catalyst bed, and the bulk (external) reactant diffusion coefficient within the catalyst bed.

The zeolite supported nickel catalysts demonstrate outstanding activity for steam reforming of *n*-hexane in the temperature range 400° to 500°C at 1 atm. The fine pore structure of these catalysts provides a

much greater limitation on mass transport via pore diffusion and a predominance of heat transfer at the external surface of the catalyst pellets in contrast to the more conventional nickel alumina catalyst.

### ACKNOWLEDGMENT

The author expresses appreciation to the United Aircraft Corporation for support of this work and permission to publish.

### REFERENCES

1. BROOKS, C. S., *Adv. in Chem.* **102**, Vol. II, 426 (1971).
2. HIRSCHFELDER, J. O., CURTISS, C. F., AND BIRD, R. B., "Molecular Theory of Gases and Liquids." Wiley, New York, 1954.
3. SMITH, J. M., "Chemical Engineering Kinetics," Ch. 9. McGraw-Hill, New York, 1956.
4. WHEELER, A., "Catalysis" (P. H. Emmett, Ed.), Vol. II, Reinhold, New York, 1955.
5. WHEELER, A., *Adv. in Catalysis* **3**, 249 (1951).
6. SATTERFIELD, C. N., "Mass Transfer in Heterogeneous Catalysis." MIT Press, Cambridge, MA, 1970.
7. MIALE, J. N., CHEN, N. Y., AND WEISZ, P. B., *J. Catal.* **6**, 278 (1966).
8. RUTHVEN, D. M., *J. Catal.* **25**, 259 (1972).
9. DAMKÖHLER, G., *Z. Physik Chem.* **A193**, 16 (1943).
10. PRATER, C. D., *Chem. Eng. Sci.* **3**, 234 (1958).
11. HUTCHINGS, J., AND CARBERRY, J. J., *Amer. Inst. Chem. Eng. J.* **12**, 20 (1966).
12. CARBERRY, J. J., *I. E. C.* **58**, (10), 40 (1966).
13. LEE, J. C. M., AND LUSS, D., *I. E. C. (Fund.)* **8**, 596 (1969).
14. Private communication.
15. LINDAUER, G. L., *Amer. Inst. Chem. Eng. J.* **13** (6), 1181 (1967).
16. TURNER, G. A., *Amer. Inst. Chem. Eng. J.* **13** (4), 678 (1967).
17. MEARS, D. E., *J. Catal.* **20**, 127 (1971).